Supplementary Material for
Spatial Changes in Earthquake-Generated Ground Motion Observations: An Examination of Seven Small Aperture Arrays in Southern California

Debi Kilb*[1], Frank Vernon[1]
[1]Scripps Institution of Oceanography, University of California, San Diego, La Jolla, California, 92093-0225, USA
*Corresponding author: dkilb@ucsd.edu

Contents of this file

Appendix A: Mapped spatial distributions of the seven small aperture arrays (Figures A1–A7)
Tables S1–S5
Figures S1–S9

Introduction

This document includes station-location maps for each of the seven small aperture arrays (Appendix A), supporting data tables (Tables S1–S5), and supporting figures (Figures S1–S9) referenced in the main text.

Appendix A: Mapped Spatial Distributions of the Seven Small Aperture Arrays.

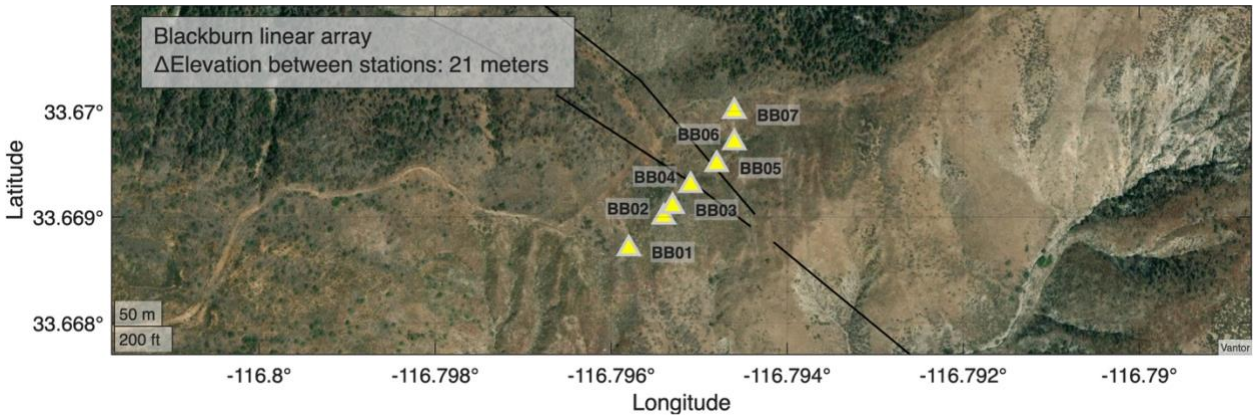

Figure A1. Mapped distribution of the Blackburn (BB) networks seismic stations.

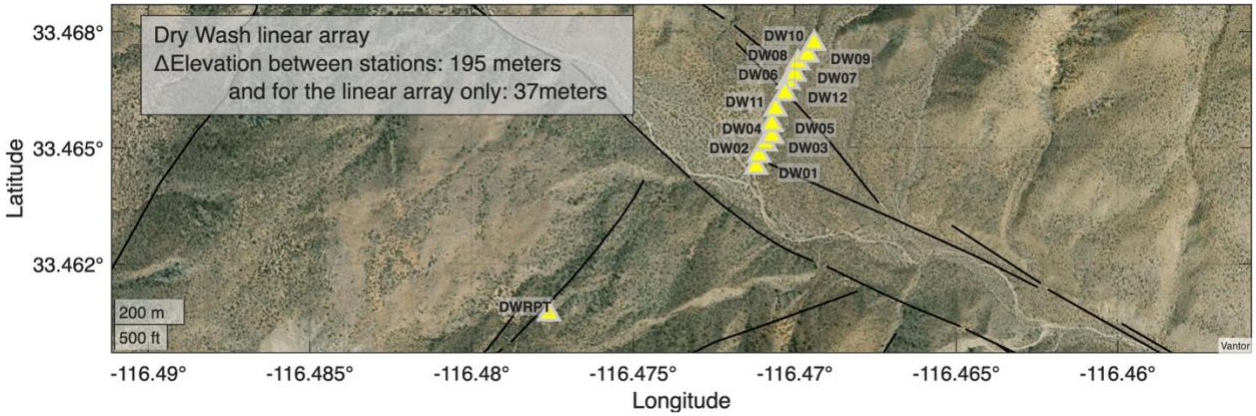

Figure A2. Mapped distribution of the Dry Wash (DW) networks seismic stations.

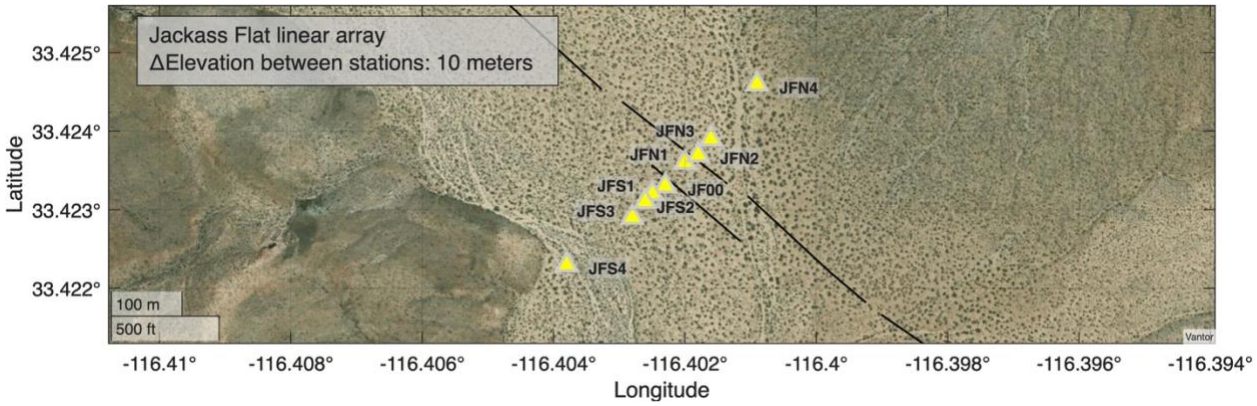

Figure A3. Mapped distribution of the Jackass Flat (JF) networks seismic stations.

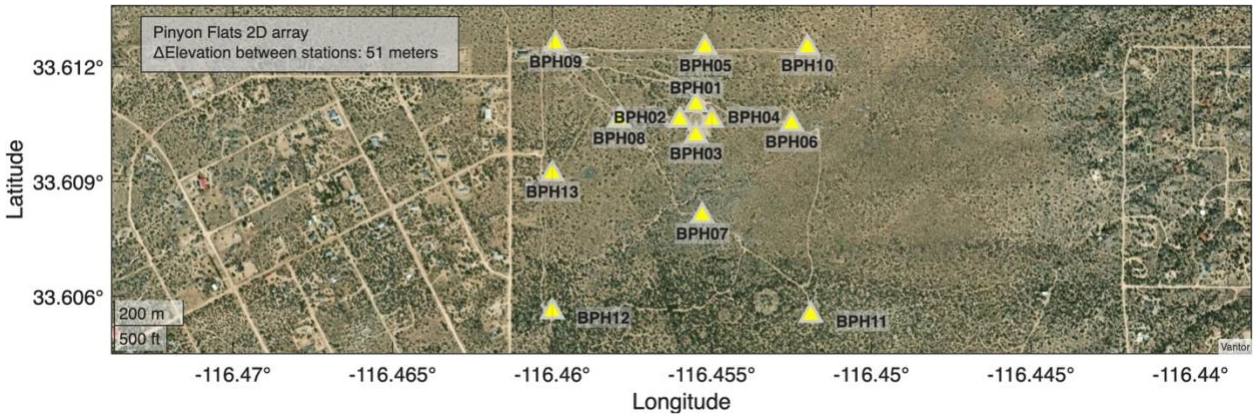

Figure A4. Mapped distribution of the Pinyon (PY) array network seismic stations.

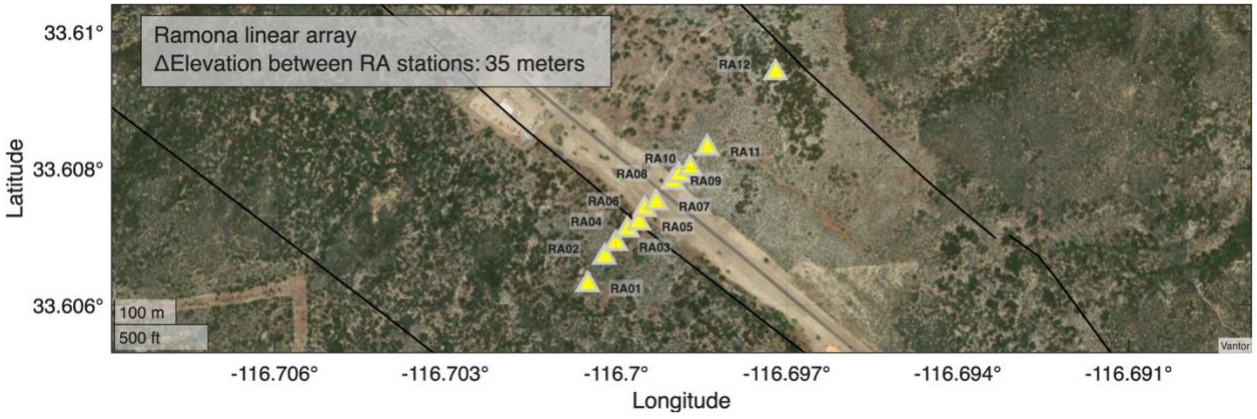

Figure A5. Mapped distribution of the Ramona (RA) array network seismic stations.

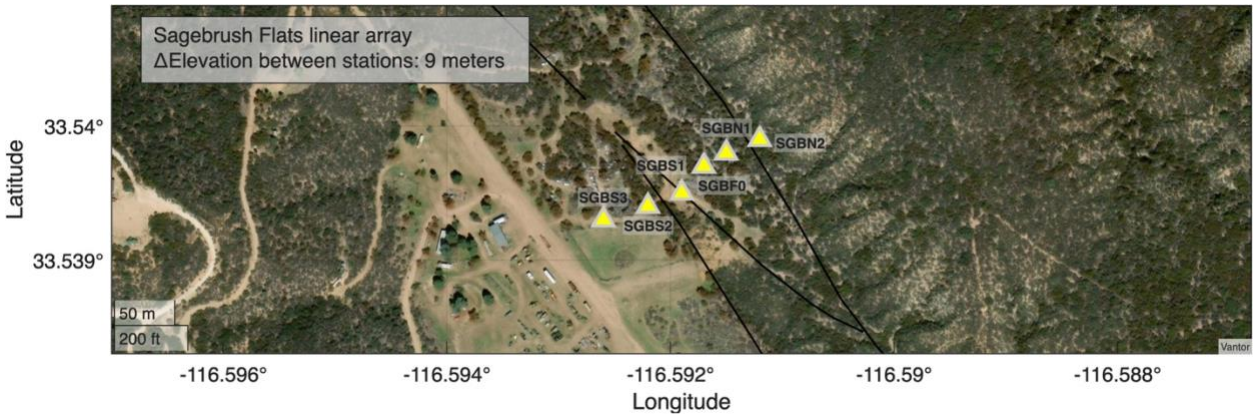

Figure A6. Mapped distribution of the Sagebrush Flat (SG) array network seismic stations. Note that stations SGBF0 and SGBFA (not labeled) are co-located but at different depths (SGBF0 is at an elevation of 1434; SGBFA is a borehole station at an elevation of 1432 meters).

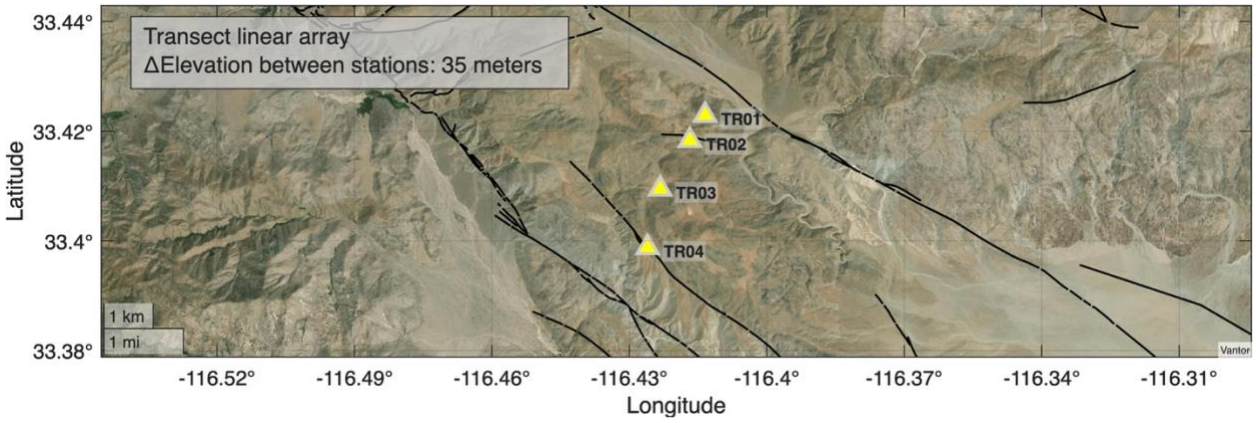

Figure A7. Mapped distribution of the Transect (TR) array network seismic stations.

Supplemental Tables.

Table S1. Data used in this study. All arrays have network codes YN except for the Pinyon Flat array that has network code PY. Station codes stand for Jackass Flat (JF), Ramona (RA), Transect (TR), Pinyon Flat (YN), Blackburn (BB), Sage Brush Flat (SG), and Dry Wash (DW). Three of these networks are still operational (YN.RA*, PY.BP*, and YN.SG*), but we only consider data through 30 June 2023 for this project. The number of earthquakes and waveforms includes only data that have passed data quality tests (i.e., overprinting, SNR, and viable signal). The SG dataset includes an M_L 4.6 earthquake near Ocotillo, CA, that occurred in 2010 (04-Nov-2010 19:39:59), prior to the deployments of the other six networks.

Net.Sta	Deployment Start Date	Deployment End Date	Duration (years)	Number of earthquakes	Number of waveforms	Magnitude Range	Depth Range (km)
YN.BB*	2012-11-22	2014-07-10	1.6	242	4986	2.5-4.4	-1-19
YN.JF*	2011-11-12	2016-11-15	5	773	20336	2.5-4.5	-1-24
YN.RA*	2012-08-11	–	11	1813	55649	2.5-4.5	-1-26
YN.DW*	2012-03-26	2017-10-31	5.6	913	28601	2.5-4.5	-1-24
YN.SG*	2010-10-23	–	13	1974	36966	2.5-4.6	-1-25
YN.TR*	2011-11-12	2017-10-31	6	953	11004	2.5-4.5	-1-24
PY.BP*	2014-04-11	–	9.2	1478	55621	2.5-4.5	-1-25

Table S2. Network sizes, sampling rates, geology, and elevation. Sensor codes HH* and HN* are velocity and acceleration, respectively. This list is sorted by the spatial diameter of the array, from shortest (SG network) to longest (TR network).

Network.Station (number of stations in array)	Sensor Type	Sample Rate (Hz)	Geology	Length or aperture of the array (km)	Elevation Range (meters)	Elevation differential (meters)
YN.SG* (Nsta = 7)	HN*	200	Spanning the Clark Branch of the San Jacinto Fault Zone. Middle of the M7.3 1800 rupture.	0.15	1430-1439	9
YN.BB* (Nsta = 7)	HH*	200	Spanning the Clark Branch of the San Jacinto Fault Zone. Middle of the M7.3 1800 rupture. Middle of the M6.7 1918 rupture.	0.18	1160-1110	21
YN.JF* (Nsta = 9)	HH*	200	Spanning the Clark Branch of the San Jacinto Fault Zone. Middle of the M7.3 1800 rupture.	0.37	657-667	10
YN.RA* (Nsta = 12)	HN*	200	Spanning the Clark Branch of the San Jacinto Fault Zone. Middle of the M7.3 1800 rupture. Termination of the M6.7 1918 rupture.	0.46	1467-1502	35

YN.DW* (Nsta = 13)	HH*	200	Spanning the Clark Branch of the San Jacinto Fault Zone. Middle of the M7.3 1800 rupture.	1.10	1085-1280	195 (37 for linear only; excludes DWRPT')
PY.BP* (Nsta = 13)	HH*	200	Off-fault 2D array at the Pinyon Flats Observatory.	1.10	1251-1302	51
YN.TR* (Nsta = 4)	HH*	200	Off-fault, between the Clark and Coyote Creek branches of the San Jacinto Fault Zone, southwest of the JF array.	2.90	739-774	35

67

68

Table S3. Summary of flagged outliers. We tested 213,163 waveforms that passed both the SNR and events close in time and space restrictions. Each of the 1020 waveforms flagged as outliers (either larger or smaller than expected) were examined (in both the time and frequency domain) and deemed viable or non-viable. A complete list of the flagged outliers can be found in Kilb & Vernon, 2025c. The percentage of flagged outliers for all networks was less than 1%. The 350 non-viable waveforms were removed from the catalogs and not considered in the analysis. Table is sorted by the percentage of non-viable waveforms.

Network	# Waveforms	# Flagged Waveforms (% of total)	# Viable Waveforms (% of total)	# Non-viable Waveforms (% of total)
RA	55649	391 (0.70%)	157 (40%)	234 (60%)
TR	11004	57 (0.52%)	34 (60%)	23 (40%)
JF	20336	68 (0.33%)	48 (71%)	20 (29%)
SG	36966	89 (0.24%)	48 (54%)	41 (46%)
DW	28601	72 (0.25%)	65 (90%)	7 (10%)
PY	55621	330 (0.59%)	305 (92%)	25 (8%)
BB	4986	13 (0.26%)	13 (100%)	0 (0%)
TOTAL	**213163**	**1020**	**670**	**350**

Table S4a. Events that produce the largest ground motions for each station in each network, for both PGV and PGA. See Table S1 for the magnitude range of each dataset. These are velocity sensor data, where acceleration was computed by differentiating the velocity data. To highlight that not all peak measurements were generated by the same earthquake, magnitude values are shaded in blue for events selected the most often (collectively for PGA and PGV measurements). Non-colored magnitude cells represent peak measurements generated from earthquakes out of the norm. A complete list of these findings, including dates, times, and ID numbers, can be found in the Kilb & Vernon, 2025b.

Net.Sta	PGA (g)	Depth (km)	Magnitude	EpiDist (km)	Azimuth (degree)	PGV (cm/s)	Depth (km)	Magnitude	EpiDist (km)	Azimuth (degree)
YN.BB01	0.01	16	3.08	17	116	0.2	18	3.63	19	59
YN.BB02	0.011	16	3.08	17	116	0.22	18	3.63	19	59
YN.BB03	0.012	16	3.08	17	116	0.21	18	3.63	19	59
YN.BB04	0.014	16	3.08	17	117	0.25	16	3.08	17	117
YN.BB05	0.01	16	3.08	17	117	0.23	16	3.08	17	117
YN.BB06	0.025	16	3.08	17	117	0.41	16	3.08	17	117
YN.BB07	0.016	16	3.08	17	117	0.3	16	3.08	17	117
YN.JF00	0.024	13	3.37	13	284	0.84	17	4.39	76	323
YN.JFN1	0.019	13	3.37	13	283	0.70	17	4.39	76	323
YN.JFN2	0.02	13	3.37	13	282	0.70	17	4.39	76	323
YN.JFN3	0.019	13	3.37	13	282	0.56	17	4.39	76	323
YN.JFN4	0.019	13	3.37	13	279	0.56	13	3.37	13	279
YN.JFS1	0.019	13	3.37	13	284	0.67	17	4.39	76	323
YN.JFS2	0.017	13	3.37	13	284	0.63	17	4.39	76	323
YN.JFS3	0.017	13	3.37	13	285	0.55	17	4.39	76	323
YN.JFS4	0.011	13	3.37	13	288	0.41	17	4.39	76	323

YN.DW01	0.013	11	2.95	12	98	0.21	11	2.95	12	98
YN.DW02	0.0076	13	3.59	27	134	0.13	11	2.95	12	98
YN.DW03	0.0073	11	2.95	12	99	0.14	11	2.95	12	99
YN.DW04	0.012	11	2.95	12	99	0.2	11	2.95	12	99
YN.DW05	0.013	11	2.95	12	99	0.27	11	2.95	12	99
YN.DW06	0.009	10	2.85	15	138	0.19	11	2.95	12	101
YN.DW07	0.013	10	2.85	15	139	0.19	11	2.95	12	101
YN.DW08	0.017	11	2.95	12	102	0.25	11	2.95	12	102
YN.DW09	0.017	11	2.95	12	102	0.24	11	2.95	12	102
YN.DW10	0.011	11	2.95	12	103	0.19	11	2.95	12	103
YN.DW11	0.0094	13	3.59	28	134	0.19	11	2.95	12	100
YN.DW12	0.012	13	3.59	28	134	0.2	13	3.59	28	134
YN.DWRPT	0.013	11	2.95	12	92	0.22	11	2.95	12	92
YN.TR01	0.024	9	3.37	80	110	0.49	17	4.39	76	324
YN.TR02	0.018	13	3.80	16	164	0.28	13	3.80	16	164
YN.TR03	0.015	13	3.80	15	158	0.25	13	3.59	21	129
YN.TR04	0.020	13	3.80	15	153	0.54	6	3.61	11	166
PY.BPH01	0.043	10	3.60	17	204	0.64	10	3.60	17	204
PY.BPH02	0.041	11	3.49	17	210	0.63	11	3.49	17	210
PY.BPH03	0.041	11	3.49	17	210	0.59	11	3.49	17	210
PY.BPH04	0.042	10	3.60	17	204	0.61	11	3.49	17	209
PY.BPH05	0.032	10	3.60	18	204	0.61	10	3.60	18	204
PY.BPH06	0.017	10	3.60	17	205	0.35	10	3.60	17	205
PY.BPH07	0.026	11	3.49	17	210	0.43	11	3.49	17	210
PY.BPH08	0.068	17	2.79	112	301	0.89	17	2.79	112	301
PY.BPH09	0.045	11	3.49	17	208	0.59	11	3.49	17	208
PY.BPH10	0.026	10	3.60	18	205	0.49	10	3.60	18	205
PY.BPH11	0.024	10	3.60	17	206	0.53	10	3.60	17	206
PY.BPH12	0.013	11	3.49	17	209	0.24	11	3.49	17	209
PY.BPH13	0.035	11	3.49	17	208	0.49	11	3.49	17	208

91

Table S4b. As in Table S4a, but for acceleration sensor data. Velocity measurements were computed by integrating the acceleration data. Here, green shading is used instead of blue.

Net.Sta	PGA (g)	Depth (km)	Magnitude	EpiDist (km)	Azimuth (degree)	PGV (cm/s)	Depth (km)	Magnitude	EpiDist (km)	Azimuth (degree)
YN.SBF0	0.02	14	3.86	21	120	0.59	13	4.15	37	239
YN.SBFA	0.0058	13	4.15	37	239	0.23	13	4.15	37	239
YN.SBN1	0.025	13	4.15	37	239	0.79	13	4.15	37	239
YN.SBN2	0.023	13	4.15	37	239	0.82	13	4.15	37	239
YN.SBS1	0.021	13	4.15	37	239	0.64	13	4.15	37	239
YN.SBS2	0.02	14	3.86	21	119	0.58	14	3.86	21	119
YN.SBS3	0.017	13	3.42	20	313	0.47	13	4.15	37	239
YN.RA01	0.015	18	3.87	23	312	0.31	18	3.87	23	312
YN.RA02	0.026	16	3.08	17	320	0.41	18	3.87	23	312
YN.RA03	0.019	12	2.80	13	302	0.45	18	3.87	23	312
YN.RA04	0.023	14	2.71	14	322	0.33	12	2.80	13	302
YN.RA05	0.013	12	2.80	13	301	0.29	18	3.87	23	312
YN.RA06	0.019	14	2.71	14	321	0.41	18	3.87	23	312
YN.RA07	0.013	12	2.80	13	301	0.40	18	3.87	23	312
YN.RA08	0.017	16	3.08	17	318	0.36	18	3.87	23	311
YN.RA09	0.012	12	2.80	13	301	0.29	18	3.87	23	311
YN.RA10	0.01	16	3.08	17	318	0.23	18	3.87	23	311
YN.RA11	0.0076	12	2.80	13	300	0.22	18	3.87	23	311
YN.RA12	0.0073	12	2.80	14	299	0.14	17	4.54	138	291

Table S5. Description of parameters in focal_swave_pgv_M3_08_vs_M3_63.csv. F_SV is the far-field SV-wave radiation pattern coefficient for a double-couple source, describing the theoretical amplitude of vertically polarized S-waves as a function of source-to-station azimuth, ray takeoff angle, and focal mechanism (strike, dip, and rake). F_SH is the equivalent coefficient for horizontally polarized S-waves. Both are derived from the focal mechanism strike, dip, and rake following Aki and Richards (2002). Values are computed at each station's azimuth and takeoff angle for each event and normalized to the median across stations to facilitate comparison of relative radiation pattern effects independent of source size.

Parameter	**Description**
station	Seismic station code
comp	Component: R = radial T = transverse (|F_SH|)
az_M308_deg	Source-to-station azimuth for M3.08 (°)
dist_epi_M308_km	Epicentral distance for M3.08 (km)
dist_hypo_M308_km	Hypocentral distance for M3.08 (km)
takeoff_M308_deg	Ray takeoff angle from source for M3.08 (°)
az_M363_deg	Source-to-station azimuth for M3.63 (°)
dist_epi_M363_km	Epicentral distance for M3.63 (km)
dist_hypo_M363_km	Hypocentral distance for M3.63 (km)
takeoff_M363_deg	Ray takeoff angle from source for M3.63 (°)
fs_comp_M308	Absolute S-wave radiation coefficient F_S for M3.08
fs_comp_M308_norm	F_S normalized to median across stations for M3.08

fs_comp_M308_pctmax	F_S as fraction of theoretical maximum for M3.08 (nodal threshold = 0.15)
fs_comp_M363	Absolute S-wave radiation coefficient F_S for M3.63
fs_comp_M363_norm	F_S normalized to median across stations for M3.63
fs_comp_M363_pctmax	F_S as fraction of theoretical maximum for M3.63 (nodal threshold = 0.15)
fs_ratio_norm	Ratio of normalized F_S: M3.08 / M3.63
pgv_M308_cms	Peak ground velocity for M3.08 (cm/s)
pgv_M308_norm	PGV normalized to median across stations for M3.08
pgv_M363_cms	Peak ground velocity for M3.63 (cm/s)
pgv_M363_norm	PGV normalized to median across stations for M3.63
pgv_ratio_obs	Ratio of observed raw PGV: M3.08 / M3.63 (no distance correction applied)

Supplemental Figures.

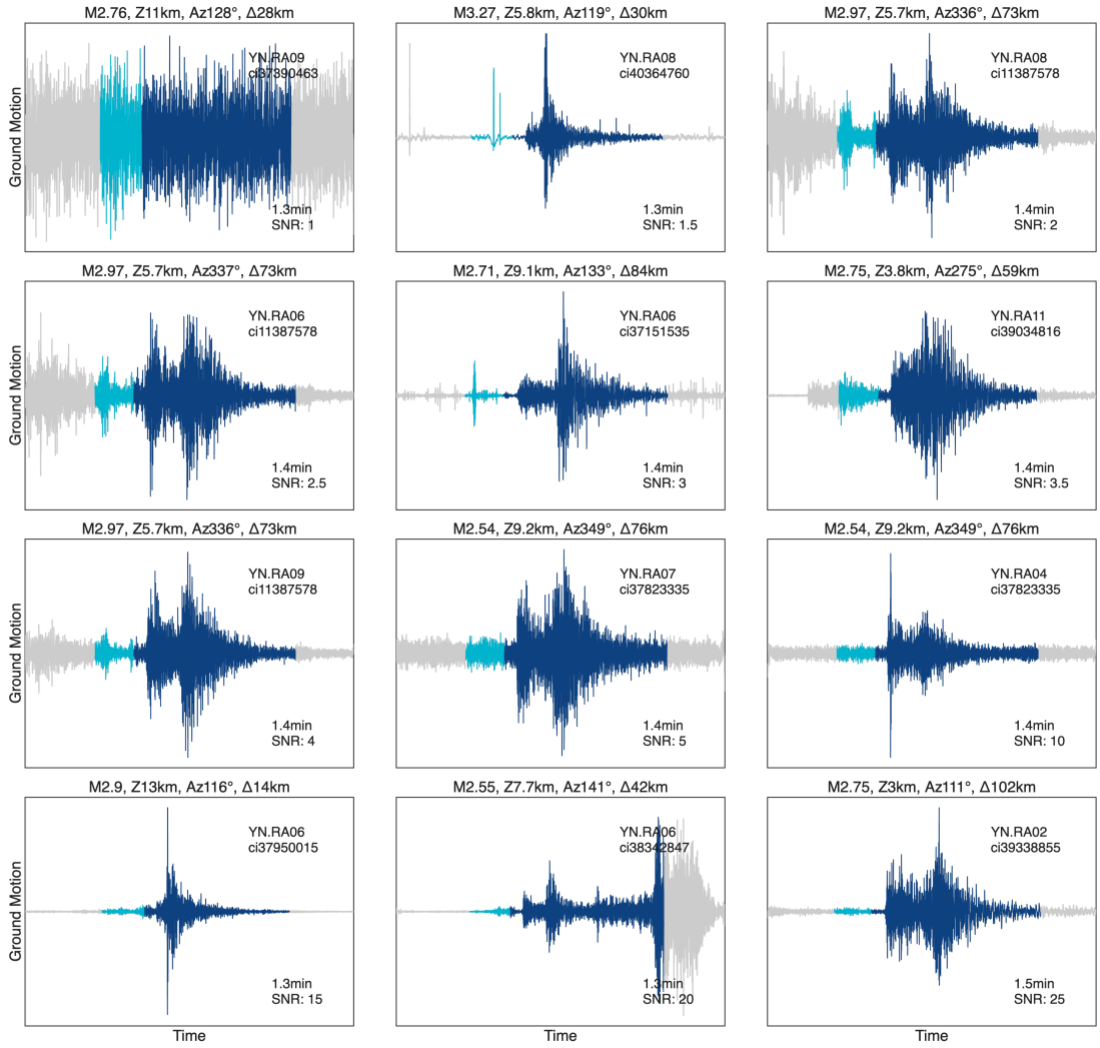

Figure S1. SNR level examples, ordered from smallest (top left) to largest (bottom right). Subtitles include the earthquake magnitude, depth, azimuth, and hypocentral distance values. Labels within each subplot, ordered from top to bottom, are network.station, earthquake ID, waveform duration, and SNR. The durations are non-uniform because they are based on the time separation between the P-wave and S-wave theoretical arrival times. The SNR is computed by taking the ratio of the largest absolute value of the data waveform (dark blue) divided by the largest absolute value of the noise waveform (light blue). Only data with SNRs

2.5+ are retained. The intermittent spike behavior at station RA04 is from local traffic on a nearby roadway.

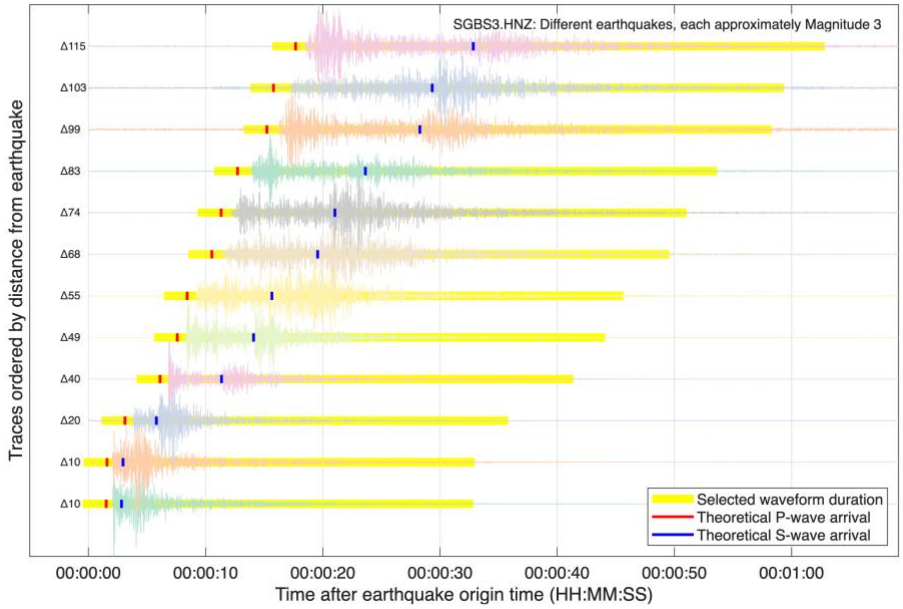

Figure S2. Examples of the variability of seismogram duration selection for ~M3 earthquakes recorded at station SGBS3.HNN. These ~M_L 3 earthquakes are located at different distances (Δ values listed on left) from the recording station. Using theoretical estimates of P-wave and S-wave arrival times (red and blue small vertical bars, respectively), we select data from 2 seconds prior to the theoretical p-wave arrival (red vertical bar) through 30 seconds after the theoretical s-wave arrival (blue vertical bar). These estimated arrival times are not exact but are sufficient for our data snippet selection purposes. Data snippet durations (yellow bar lengths) differ to account for the larger time separation between the P- and S-wave arrival times for more distant recordings.

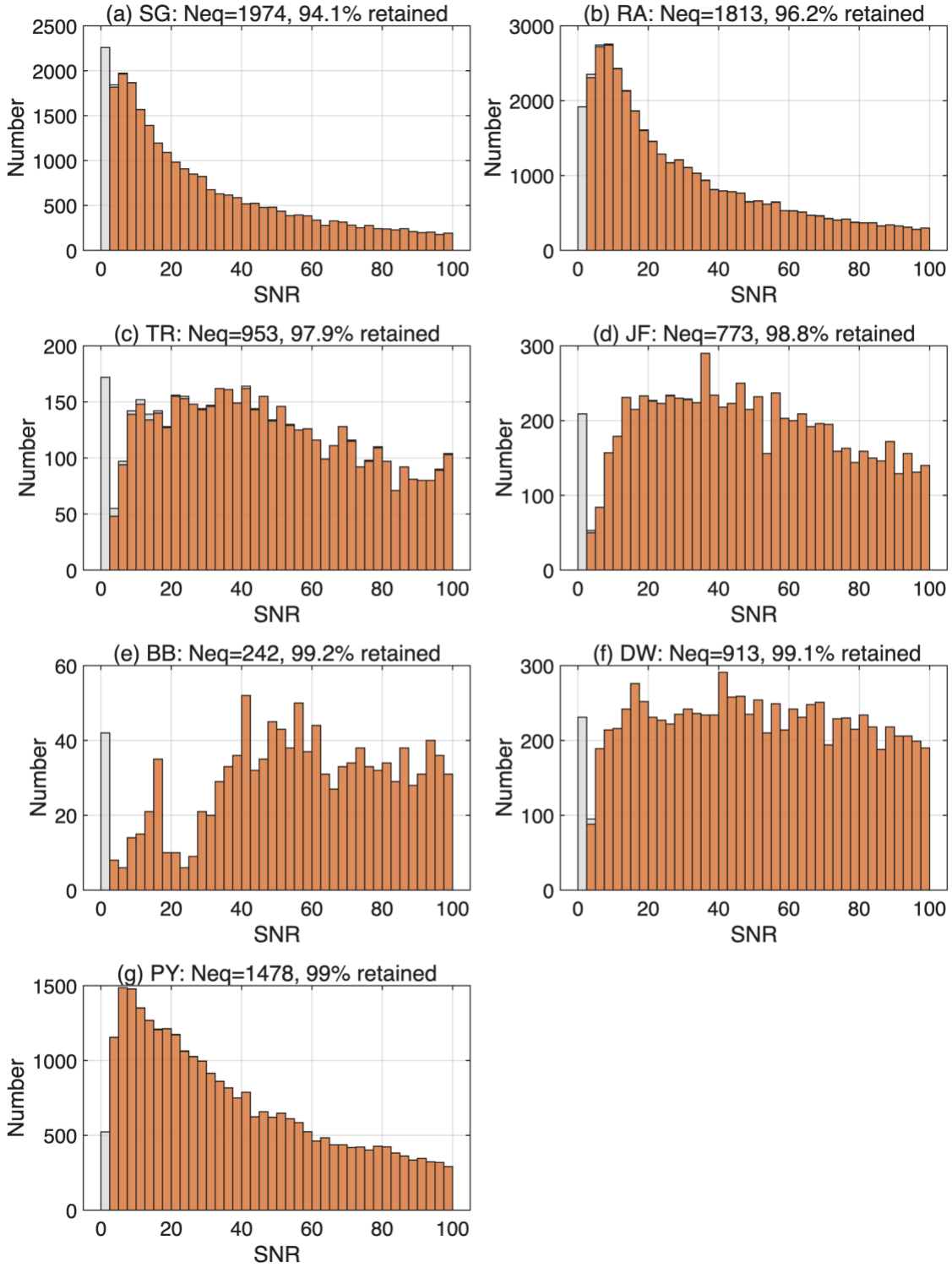

Figure S3. Summary SNR histograms for each of the seven networks. Data with SNR<2.5 (gray) are removed. The number of earthquakes tested (Neq) and the percent of earthquakes retained

after the SNR restrictions are listed in the sub-plot titles. The SG and RA networks are the most prone to SNR issues, retaining only 94.1% and 96.2% of the data, respectively. All other networks retain 97.9% or more of these data.

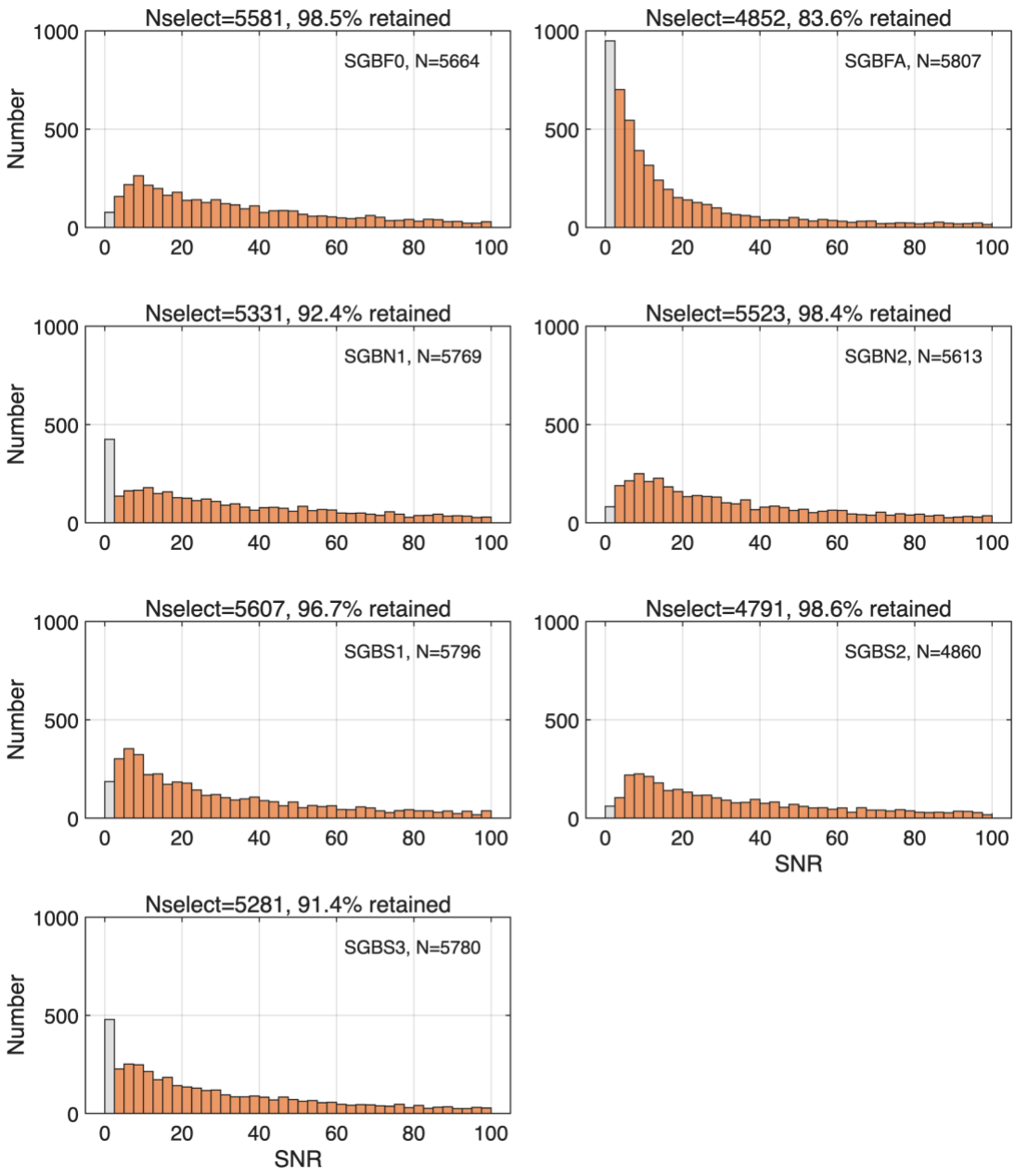

Figure S4. As in Figure S3, but for individual stations in the SG network. Y-axis scales are identical in all subplots. Stations SGBFA, SGBN1, and SGBS3 net the most SNR below the threshold value (SNR<2.5; elevated gray bars in the SGBFA, SGBN1, and SGBS3 distributions), retaining 83.6%, 92.4%, and 91.4% of these data, respectively. Stations that record the best data (i.e., 98% or more of these data retained) were SGBF0 (borehole station in the fault core), SGBN2, and SGBS2 (stations on the north side of the fault).

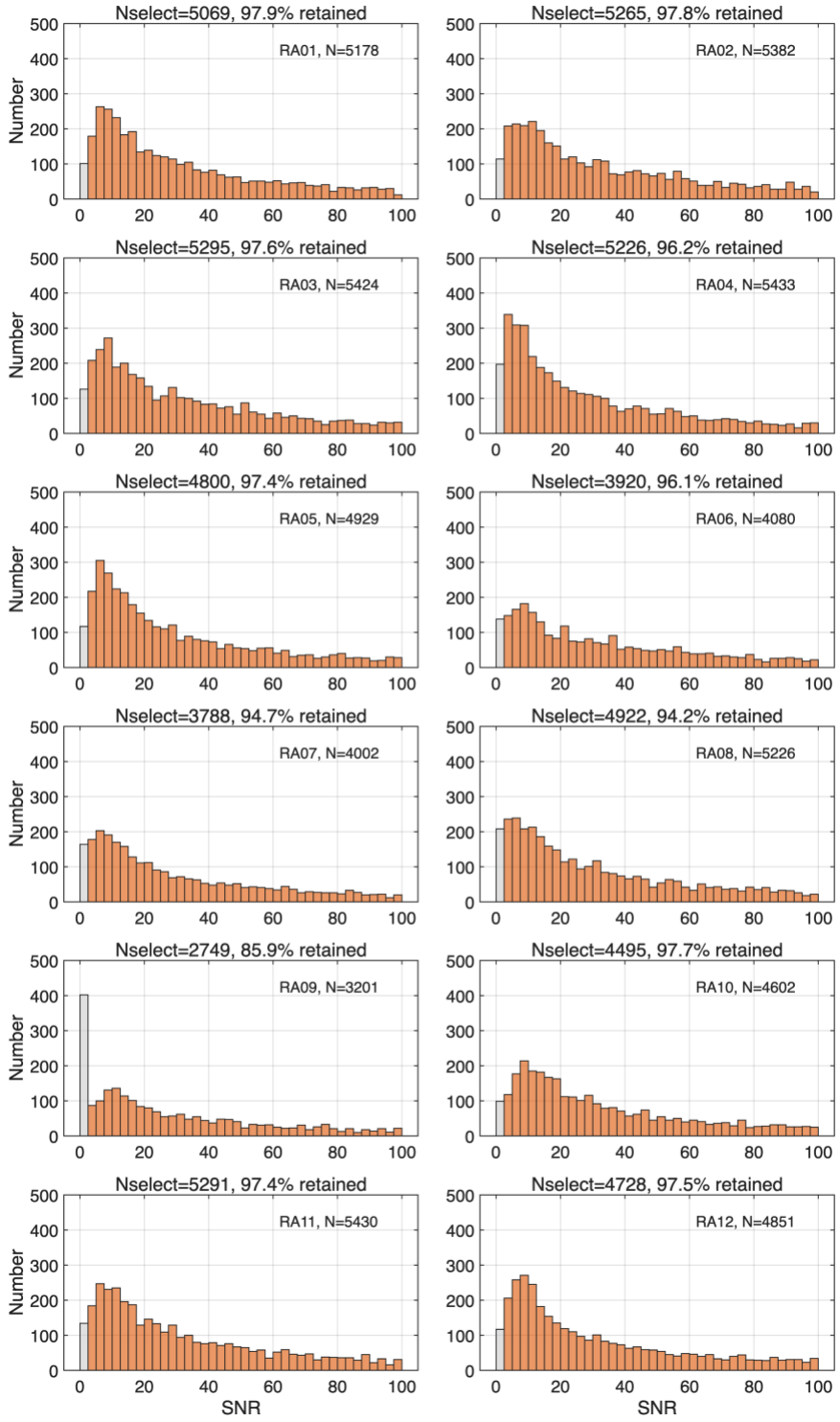

146

147 **Figure S5.** As in Figure S3, but for individual stations in the RA network. Note that station

148 RA09 has substantially more data that do not meet the SNR restriction (i.e., larger gray bar in

RA09 histogram). Only 85.9% of the RA09 data are retained. This stems from instrumental issues in late 2015 through early 2016 and is the correct behavior. All other RA stations retain 94.2% of these data or more.

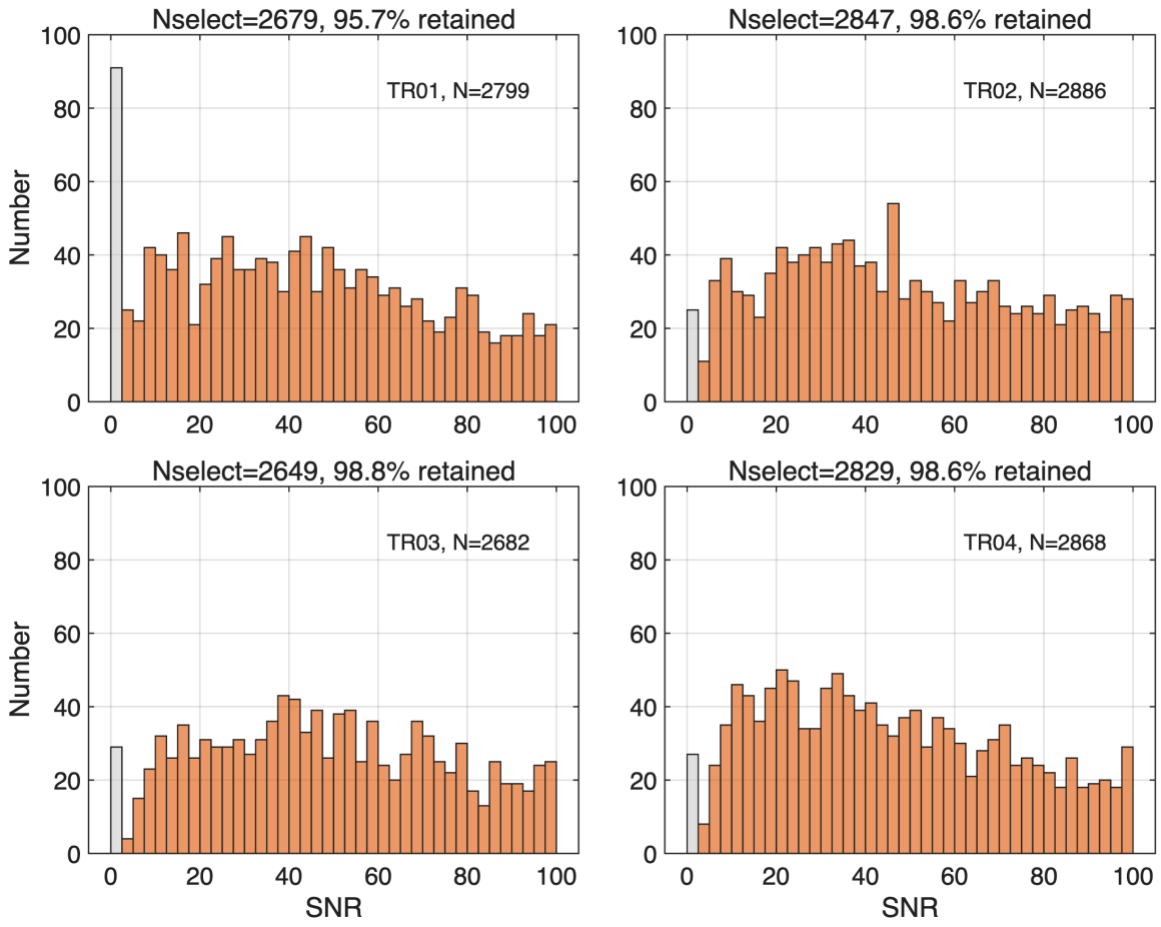

Figure S6. As in Figure S3, but for individual stations in the TR network. Station TR01 has substantially more data that do not meet the SNR restriction (i.e., larger gray bar in TR01 histogram) that is caused by two periods of elevated instrumental noise issues at this station in ~2015 and ~2017.

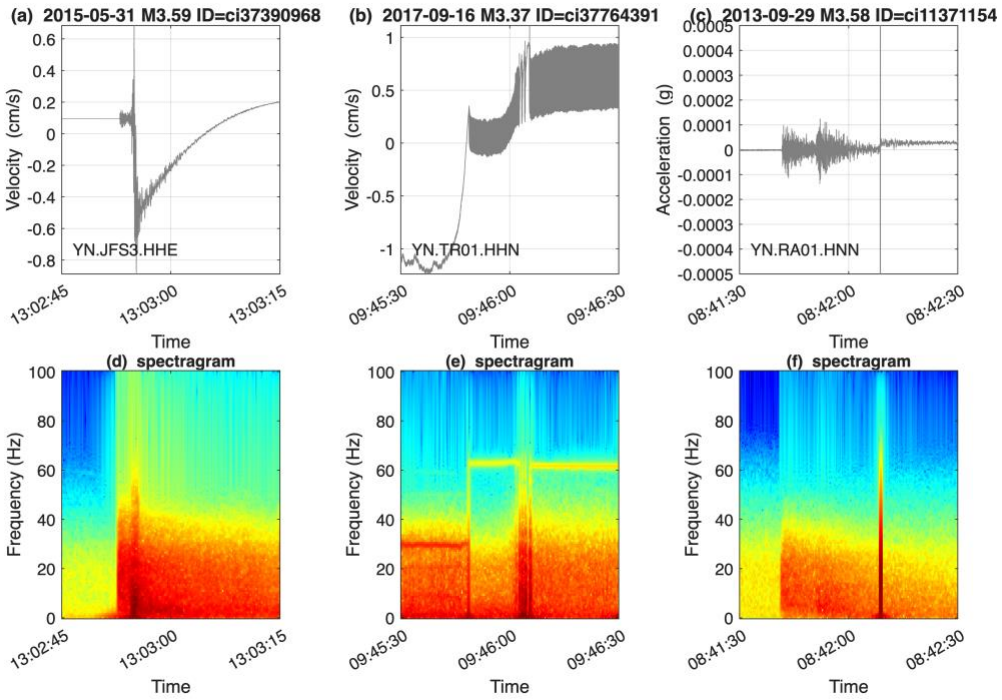

Figure S7. Examples of signals flagged as non-seismic and removed from the catalogs. These include time-domain signals (a-c; top row) and the associated frequency-domain signals (d-f; bottom row). These examples include clipped signals (a and d), instrumental noise (b and e), and a data spike (c and f).

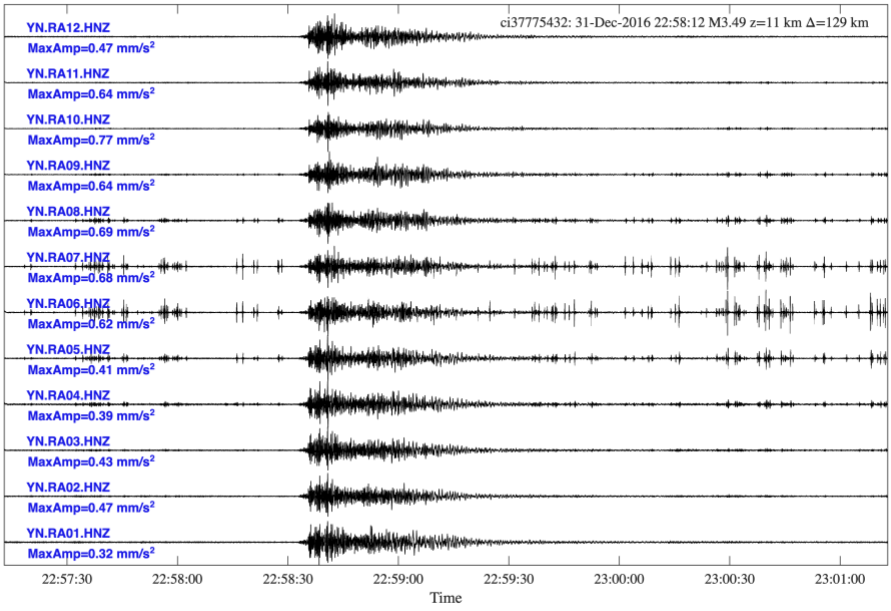

167

168 **Figure S8.** An example of car traffic signals recorded by the RA array, which traverses the Table
169 Mountain Truck Trail road along the San Jacinto Fault Zone. The prevalent spike signals
170 recorded by stations closest to the road/fault (RA08, RA07, RA06, and RA05) are the signature
171 of passing cars. The car traffic spikes are less pronounced for stations farther from the roadway
172 (stations RA01, RA02, RA03, RA04, RA09, RA10, RA11, RA12).

173

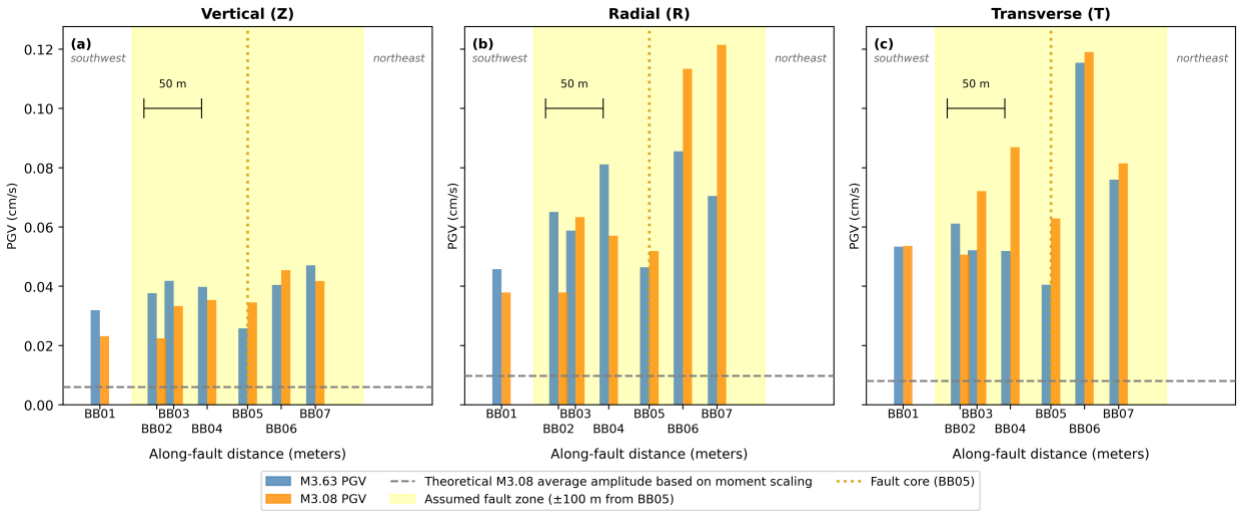

Figure S9. Peak ground velocity (PGV) for M3.63 (blue) and M3.08 (orange) events recorded at BB array stations, plotted at their true along-fault positions relative to the assumed fault core (BB05, vertical dotted line). The yellow band marks the assumed fault zone (±100 m from BB05). BB01 lies outside this zone. The dashed line shows the theoretically expected M3.08 amplitude derived from the mean M3.63 distance-corrected PGV scaled by the moment ratio (×1/6.7). All three panels share the same vertical axis scale to highlight the lower absolute amplitudes on the vertical component. On the radial and transverse components, M3.08 amplitudes approach or exceed those of the M3.63 from BB03 northeastward, despite M3.08 being the smaller event.